Open access • Posted Content • DOI:10.1101/2020.01.29.926196

Analysis of metagenome-assembled genomes from the mouse gut microbiota reveals distinctive strain-level characteristics — Source link

Shenghui Li, Shenghui Li, Siyi Zhang, Bo Li ...+17 more authors

Institutions: Dalian Medical University, Genentech

Published on: 31 Jan 2020 - bioRxiv (Cold Spring Harbor Laboratory)

Topics: Gut flora, Firmicutes and Akkermansia muciniphila

Analysis of metagenome-assembled genomes from the mouse gut microbiota reveals distinctive strain-level characteristics

Shenghui Li[1,2#], Siyi Zhang[3#], Bo Li[1,3#], Shanshan Sha[3], Jian Kang[3], Peng Li[2], Aiqin Zhang[2], Qianru Ji[2], Qingbo Lv[4], Xiao-Xuan Zhang[4], Hongbo Ni[4], Xiuyan Han[1,3], Miao Xu[1,3], Guangyang Wang[1,3], Wenzhe Zhang[1,3], Yuanyuan Sun[1,3], Roujia Xu[1,3], Yi Xin[5], Qiulong Yan[1*], Yufang Ma[1,3*]

[1].Department of Microbiology, College of Basic Medical Sciences, Dalian Medical University, Dalian, China.

[2]. Shenzhen Puensum Genetech Institute, Shenzhen, China.

[3].Department of Biochemistry and Molecular Biology, College of Basic Medical Sciences, Dalian Medical University, Dalian, China.

[4].College of Animal Science and Veterinary Medicine, Heilongjiang Bayi Agricultural University, Daqing, Heilongjiang Province 163319, PR China.

[5]. Department of Biotechnology, College of Basic Medical Sciences, Dalian Medical University, Dalian, China.

[*]Correspondence: Yufang Ma (yufang_ma@hotmail.com) & Qiulong Yan (qiulongy1988@163.com)

[#]These authors have contributed equally to this work.

Abstract

The laboratorial mouse harbors a unique gut microbiota with potential value for human microbiota-associated studies. Mouse gut microbiota has been explored at the genus and species levels, but features rarely been showed at the strain level. The identification of 833,051 and 658,438 nonredundant genes of faeces and gut content samples from the laboratorial C57/BL mice showed over half of these genes were newly found compared to the previous mouse gut microbial gene catalogue. Metagenome-assembled genomes (MAGs) was used to reconstruct 46 nonredundant MAGs belonging to uncultured specieses. These MAGs included members across all phyla in mouse gut (i.e. Firmicutes, Bacteroidetes, Proteobacteria,

Deferribacteres, Verrucomicrobia, and Tenericutes) and allowed a strain-level delineating of the mouse gut microbiota. Comparison of MAGs with human gut colonies revealed distinctive genomic and functional characteristics of mouse's Bacteroidetes and Firmicutes strains. Genomic characteristics of rare phyla in mouse gut microbiota were demonstrated by MAG approach, including strains of *Mucispirillum schaedleri*, *Parasutterella excrementihominis*, *Helicobacter typhlonius*, and *Akkermansia muciniphila*.

Importance

The identification of nonredundant genes suggested the existence of unknown microbes in the mouse gut samples. The metagenome-assembled genomes (MAGs) instantiated the specificity of mouse gut species and revealed an intestinal microbial correlation between mouse and human. The cultivation of faeces and gut contents sample validated the existence of MAGs and estimate their accuracy. Full-length 16S ribosomal RNA gene sequencing enabled taxonomic characterization. This study highlighted a unique ecosystem in the gut of laboratorial mice that obviously differed with the human gut flora at the strain level. The outcomes may be beneficial to researches based on laboratorial mouse models.

Introduction

The gut microbiota is a dense and diverse ecosystem (1). The associations between altered gut microbial composition and various pathogenesis, such as obesity (2, 3), type 2 diabetes (4), rheumatoid arthritis (5), and allergy (6), has become a research hotspot. Murine models, especially mouse, are widely used in biomedical study. Many studies have showed that mouse intestinal models also play a pivotal role in human gut microbial research. Some phyla in mouse intestinal flora, such as Firmicutes, Bacteroidetes, Proteobacteria, has resemblances with that in human (7, 8). In addition, there are plenty of similarities in anatomy, genetics and physiology between mouse and human (9). These features make the mouse one of the most essential model animals in laboratory. However, mouse gut microbiota could be influenced by many factors, including diet, ambient temperature and cleanliness. Hence, there are still some distinctions between human and mouse gut microbiota. Previous studies have showed that over 50% of genera in mouse gut microbiota are not found in human gut (10, 11). Some human gut-dominant genera, including *Faecalibacterium*, *Prevotella*, and *Ruminococcus*, rarely occurred in the mouse gut microbiota, whereas the mouse gut-dominant genera, such as *Lactobacillus*, *Turicibacter*, and *Alistipes*, were underrepresented in human intestinal flora (9).

Although there are some recent researches concerning bacterial mutations in laboratory mouse (12), few studies had focused on strain-level characteristics of laboratory mouse gut microbiota. In this study, using a metagenome-assembled genome (MAG) approach, we analyzed the microbial genomes that were obtained from laboratorial mouse gut microbiota, and revealed distinctive genomic and functional features of these genomes at the strain level. Our findings suggested a conceivable unique ecosystem in laboratorial mice gut and might benefit the research fields with applications to such model organisms.

Results

Microbial contents in the mouse intestinal tract

To investigate the overall gut microbial composition of laboratorial mouse, we collected the faeces and gut content samples from three male C57/BL mice and generated a total of 33.9 Gbp high-quality data (5.7±0.5 Gbp per sample, **Table S1**) via whole-metagenome shotgun sequencing. *De novo* assembly and gene prediction of these metagenomic data generated two nonredundant protein-coding gene catalogues for the faeces and gut content samples, containing 833,051 (average length, 695bp) and 658,438 (average length, 708bp) genes, respectively. Over 50% of genes were shared between two body sites (**Figure 1A**), in agreement with the previous studies showing an enormous commonality of microbial content of different intestinal tract sites (13). When combined with the most comprehensive nonredundant catalogue (representing ~2.4 million genes) established by 184 mice faecal samples from overall the world (14), the current mouse gut microbial gene catalogue therefore contained ~2.8 million genes (**Figure 1A**). A high proportion of new genes (52.2%) in this study might be due to more data amounts per sample, improved assembly methods, as well as the population-specific signatures of the mouse intestinal microbiota (14, 15). This combined gene catalogue allowed an average of 73% reads mapping rate for current sequenced samples, and the remaining reads were generally derived from non-coding zone or unassembled sequences. Notably, based on taxonomic annotation via the NCBI-nt database, 63.6% genes in the mouse gut catalogue could be classified at the phylum level, however, only 8.4% genes could be assigned into a genus and only 6.0% genes could be assigned into a species (**Figure 1B**). At the phylum level, the dominant phylum in mouse intestinal samples were Bacteroidetes (average relative abundance = 28.5%), Firmicutes (23.2%), Proteobacteria (18.4%), Deferribacteres (12.3%) and Verrucomicrobia (4.7%), while at the phylum-level unclassified genes consisted an average of 12.3% abundance in all samples. At the genus level, however, an

average of 51.8% sequences of the samples were assigned into the genus-level unclassified genes, and the remaining sequences were generally dominated by Parabacteroides (average relative abundance = 10.6%), Helicobacter (7.6%), Lactobacillus (7.5%), Mucispirillum (6.6%) and diverse genera belonging to other phyla (**Figure 1B**). Taken together, these findings highlight the incomplete coverage of mouse gut microbial genes and taxonomic information in current knowledge. We compared the mouse gut microbial gene catalogue to two comprehensive gene catalogues of the human (9.9 million genes constructed from 1,267 individuals (16)) and rat (5.1 million genes constructed from 98 rats (17)). Only 19.2% genes in the mouse gut microbiotawere also observed in the rat catalogue gut, and only 4.6% genes were shared with the human catalogue (**Figure 1C**). This closer relationship between mouse and rat gut microbiota would be explained by their physiological connections and similar ecological habit, despite that, the low proportion of shared genes between mouse and rat/human gut suggested a unique ecosystem in laboratorial mice.

Strains resolving of the mouse gut microbiota based on metagenomic-assembled genomes

Recent development of computational techniques allowed us to identify the draft genomes of a portion of uncultivated species in highly diverse metagenomic samples (18, 19). To characterize the microbial strains in mouse intestinal microbiota, we recovered the MAGs for each sample from their assembled contigs (see Materials and Methods for details), which was represented by a total of 236,108 contigs with minimum length of 1.5 kbp (total length of 1.0 Gbp). A total of 112 MAGs were obtained from all samples under strict quality criteria of estimated completeness >70% and contamination <5%. Then, 55 unique MAGs were generated after removing redundancy (**Table S2**), of which 31 MAGs met the standard of high-quality draft genomes (completion >90% and contamination <5%) (**Figure 2A**). These MAGs consisted of 265 scaffolds in average (range from 33 to 760) with an average N50 length of 70 kbp (ranging from 4.2 to 348 kbp), and had an average of sequencing coverage of 96.2X (ranging from 8.1X to 604X). Notably, these 55 MAGs showed distinct genomic similarity with pairwise average nucleotide identity (ANI) ranging from 43% to 95% (average 48%, Figure 2), and captured approximately 50.6% of sequencing reads in all metagenomic-sequenced faecal and gut content samples (**Table S1**), representing a strain-level resolving of the mouse intestinal microbiota.

We applied both marker gene-based and whole genome-based approaches to determinate the taxonomic placement of these 55 MAGs. Expectedly, the largest number of strains was from Firmicutes (41.8%, 23/55),

Bacteroidetes (40%, 22/55) and Proteobacteria (12.7%, 7/55) (**Figure 2A; Table S2**). And the other strains belonged to relatively low abundance phyla Deferribacteres (n =1), Verrucomicrobia (1) and Tenericutes (1). At the lower taxonomic levels, however, only 9 (16.4%) strains could be robustly assigned to known species, and the remainsing were novel candidate species that were classified into known bacterial genera, families or orders (**Table S2**).

To validate the existence of MAGs and estimate their accuracy, we isolated 13 bacterial colonies via cultivation of a mixed sample from three mice's faeces and gut contents. Full-length 16S ribosomal RNA gene sequencing was performed on all colonies to enable taxonomic characterization (**Table S3**). The majority of the colonies were members of Gammaproteobacteria and Bacilli, including 4 *Escherichia spp*., 2 *Streptococcus spp*. and 2 *Lactococcus spp*.; these species were of relatively low abundance in the mouse gut microbiota but high cultivability in the common mediums (20). One isolate, *Lactobacillus murinus* MS13, also existed in the MAGs (MAG:BG01). Whole-genome shotgun sequencing analysis of *L. murinus* MS13 revealed an almost identical genome (ANI = 99.99%) compared with MAG:BG01 (**Figure 2B**), confirming that these two genomes were derived from the same strain.

Distinctive characteristics of mouse's Bacteroidetes and Firmicutes strains compared to human's

To investigate the genomic characteristics of the two phyla, we compared our mouse MAGs with 206 strains cultivated from the gastrointestinal tract of healthy adult humans (21) (**Figure 3A; Table S4**). In spite of different gene composition, both mouse and human gut microbiota were dominated by two phyla, Bacteroidetes and Firmicutes (10). The mouse Bacteroidetes strains showed significant reductions of genome size and number of genes, and a significant increase of GC content compared to human Bacteroidetes strains (**Table 1**). In contrast, no significant changes of these parameters were detected between mouse and human Firmicutes strains.

To characterize the functional potential of the mouse gut strains, we analyzed the functional profiles of Bacteroidetes and Firmicutes of mouse MAGs and compared them with the corresponding strains of human gut. Consistent with the genomic parameters, the composition of KEGG (Kyoto encyclopedia of genes and genomes (22)) orthologs (KOs) of mouse Bacteroidetes strains demonstrates clear separation from human's (R^2 = 0.28, *adonis P*< 0.001; **Figure 3B**), whereas their Firmicutes strains were largely overlapped in KO profiles (R^2 = 0.039, *adonis P* = 0.01). The mouse Bacteroidetes strains encoded a higher density of enzymes

involving genetic information processing compared to human Bacteroidetes strains (average proportion of genes: 20.7% vs. 16.4%, $P = 1.2 \times 10^{-11}$), and the mouse Firmicutes strains encoded a higher density of enzymes involving cellular processes (average proportion of genes: 12.6% vs. 8.3%, $P = 8.5 \times 10^{-10}$); whereas strains of the two phyla in mouse gut encoded significantly lower numbers of metabolism-associated enzymes than human strains ($P = 4.5 \times 10^{-7}$ for Bacteroidetes strains and $P = 3.8 \times 10^{-8}$ for Firmicutes strains). Such deviation between mouse and human microbial strains was also observed in the low level KEGG pathways, for which 45% (112/248) pathways in Bacteroidetes strains and 23% (63/278) pathways in Firmicutes strains were significantly differed in occurance rates between mouse and human (**Table S5**). As a prominent example, the mouse Firmicutes strains were significantly enriched in pathways of flagella assembly and bacterial chemotaxis compared to human Firmicutes strains (**Figure 3C**).

Consistently, comparison of carbohydrate active enzymes (CAZymes) (23) between mouse MAGs and human strains also revealed significant differences between mouse and human derived Bacteroidetes strains ($R^2 = 0.27$, *adonis* $P < 0.001$), but no significant differences for Firmicutes strains ($R^2 = 0.013$, *adonis* $P = 0.07$). Detailedly, a large proportion (37.5%) of glycoside hydrolases, which were involved hydrolysis and/or rearrangement of glycosidic bonds, were lacked in the mouse Bacteroidetes strains compared to humans' (**Table S6**).

Characteristics of other representative strains in the mouse gut microbiota

To study the features of the mouse gut microbes belonging to the other phyla except Bacteroidetes and Firmicutes, we analyzed the genomic characteristics of four MAGs: *Mucispirillum schaedleri* MAG:AF02 from Deferribacteres, *Parasutterella excrementihominis* MAG:CG14 and *Helicobacter typhlonius*MAG:AF12 from Proteobacteria, and *Akkermansia muciniphila* MAG:BG08 from Verrucomicrobia.

Mucispirillum schaedleri MAG:AF02 consisted of 47 contigs with total length of 2.32 Mbp (N50 length:166 kbp). This MAG was very similar to the genome of *M. schaedleri* ASF457 with 99.1% ANI (**Figure 4A**), a strain that was isolated from the mucus layer of gastrointestinal tract of laboratory rodents(24).

Helicobacter typhlonius MAG:AF12 contained 33 contigs with total length of 1.87 Mbp (N50 length: 237 kbp). The closest genome of MAG:AF12 was *H. typhlonius* mit97-6810 with ANI of 99% (**Figure 4B**).

174 *Parasutterella excrementihominis* MAG:CG14 contained 397 contigs with total length of 1.59 Mbp.
175 The closest genome of MAG:CG14 was *Sutterella* sp. KGMB03119 with ANI of 96.4% (**Figure 4C**),
176 suggesting that *P. excrementihominis* MAG:CG14 was a potential new sub-species of the genus
177 *Parasutterella*.
178 *Akkermansia muciniphila* MAG:BG08 contained 216 contigs with total length of 2.55 Mbp. The closest
179 genome of MAG:BG08 was *A. muciniphila* ATCC BAA-835 which was isolated from the human intestinal
180 mucus layer (25), with ANI of 97.7% (**Figure 4D**). This result suggested potentially shared *A.muciniphila*
181 species between mouse and human gut microbiota.
182
183 **Discussion**
184 In this study, we compared the mouse gut microbial gene catalogue with that of human and rat, and analyzed
185 the mouse gut microbiota at the strain level based on the metagenome-assembled genome approach. We
186 identified the draft genomes of a portion of uncultivated species from mice faeces and gut content samples.
187 We obtained 55 unique MAGs and 31 of them met the standard of high-quality draft genomes (completion
188 >90% and contamination <5%). Since both mouse and human gut microbiota were dominated by
189 Bacteroidetes and Firmicutes (26, 27), we analyzed these two phyla at the strain level in both, and
190 characterized the potential function of mouse strains through KEGG orthologs and carbohydrate active
191 enzymes. Furthermore, we detected other phyla except Bacteroidetes and Firmicutes, and discovered that
192 some of them have the closest genome with the strains in intestinal mucus layer of laboratory rodents. These
193 outcomes suggested a unique ecosystem in the intestinal tract of laboratorial mice.
194 According to previous studies, Firmicutes was of the highest abundance in mouse gut microbiota
195 accounting for over 50%, followed by Bacteroidetes, and Deferribacteres and Tenericutes(28). The intestinal
196 bacterial community in mice with acute inflammation may alter with reduced abundance of Firmicutes and
197 Bacteroidetes, especially the clusters Clostridium XIVa and IV (29). Compared with healthy controls,
198 however, Enterobacteriaceae and other clustered groups in the Bacteroidetes may have higher abundance
199 (30-32). Compared to gut microbiota in mouse, the community in human intestinal tract is consistently
200 dominated by Firmicutes and Bacteroidetes. 95% of the Firmicutes sequences are clustered to Clostridia
201 class (10), while most of subspecies of Firmicutes related to butyrate-producing are clustered to clostridial
202 groups IV, XIVa, and XVI (33, 34). In addition, it has been reported that in rat gut microbiota, two phyla

Firmicutes and Bacteroidetes have higher abundance, followed by Proteobacteria (17). These outcomes mentioned above are concordant with our findings. Furthermore, we found that 51.8% sequences of our samples belonged to genus-level unclassified genes and the rest of sequences were *Parabacteroides*, *Helicobacter*, *Lactobacillus* and *Mucispirillum*.

Although all specieses we found are assigned to known bacterial genera, families or orders, more than 80% species were classified to novel species based on MAG during our resolving procedure, such as *Acholeplasmatales* MAG:AF08 and *P. excrementihominis* MAG:CG14. It has been reported that uncultivated prokaryotes, such as bacteria, could be obtained by single-amplified genome and MAG approaches (26) and the Genomic Standards Consortium has been completed by minimum information about a MAG, which facilitate robust genomic analyses of bacterial genome (27). However, based on this consequence, the studies on strain-level microbiota in model animals could hardly be found. In addition to analysis by MAG approach, in our study, to confirm the existence of MAGs and to evaluate accuracy, we isolated 13 bacterial colonies via conventional cultivation of a mixed sample from three mice's faeces and gut contents and all colonies were treated by full-length 16S ribosomal RNA gene sequencing to enable taxonomic characterization. One isolate, *Lactobacillus murinus* MS13, was discovered to have 99.99% average nucleotide identity of its whole genome compared with *L. murinus* MAG:BG01, confirming that these two genomes were derived from the same strain.

The Bacteroidetes and Firmicutes strains of mouse gut showed distinctive functional characteristics compared to that of human gut. Firmicutes and Bacteroidetes are generally Gram-positive and Gram-negative bacteria, respectively. Compared to the single thick and homogeneous layer of Firmicutes, Bacteroidetes has a thinner layered cell wall. The peptidoglycan in the cell walls of Bacteroidetes are less than that in Firmicutes, however, there are lipopolysaccharides, phospholipids, proteins, lipoproteins in the wall of Bacteroidetes and lipids could hardly be found in cell wall of Firmicutes. As the only connection in the elements of cell wall in both two phyla, the chemical composition of peptidoglycan in Bacteroidetes is difficult to be effected(35), in contrast, that of peptidoglycan in Firmicutes could be influenced and variable(36). Thus, this characteristic of peptidoglycan might make Bacteroidetes and Firmicutes dominant in gut microbiota, so as in mouse gut. These pathways of two phyla might be altered when they need to adapt to mouse gut environment.

Apart from Firmicutes and Bacteroidetes, some representative strains are worthy of further study, such as *Akkermansia muciniphila*. *A. muciniphila* is an anaerobic Gram-negative bacteria (37). In previous studies, it has been discovered in the intestines of mice (38). According to our findings, *A. muciniphila* in the mouse gut might have similarities with that in human gut. As an important strain in maintaining healthy gut environment, the alterations of the abundance of *A. muciniphila* may cause many types of diseases, such as type 1 diabetes (39), inflammatory bowel disease(40), autism(41), and cancer(42).

This strain-level study based on MAG approach of mouse gut microbiota might facilitate the development of animal models with more stable physiological performance, benefit clinic diagnosis and therapy and improve the reliability of mouse models. The idea of this research can be applied to many other model organisms, and is of great significance to the selection of organism models and these findings can simulate pathological status of disease more scientifically.

Materials and Methods

Experimental models and sample collection

The C57/BL mice were acquired from specific pathogen-free (SPF) Laboratory Animal Center of Dalian Medical University. All mice were housed under a 12:12 light: dark cycle and germ-free conditions in isolators. Animals were fed with autoclaved rodent chow and autoclaved tap water ad libitum. All procedures were performed in accordance with the Guide for the Care and Use of Laboratory Animals under an approved animal study proposal.

To harvest intestinal microbial communities from C57/BL mice, after the mice were sacrificed, the abdomen was sterilized by 75% ethanol and was dissected under sterile conditions. The gut contents and fecal samples were collected for cultivation and DNA extraction.

Microbial cultivation and identification

Both gut contents and fecal sample of 50 mg were added into 1 ml normal saline and the samples were diluted in BHI liquid medium. The diluents of 20 μl was spread out on solid medium and incubated at 37°C under aerobic and anaerobic conditions for 48 hours, respectively. Then, single colonies were picked up and transferred on fresh solid medium for bacterial purification. After being cultivated under the corresponding conditions for 48 hours, the single colony was inoculated into 8 ml liquid medium and incubated under the

same conditions. The culture of 100 µl was used for amplification of 16S rRNA gene by polymerase chain reaction (PCR).

The 16S rRNA gene was amplified by using primers: 7F 5'-AGAGTTTGATYMTGGCTCAG-3'and 1510R 5'-ACGGYTACCTTGTTACGACTT-3' and the PCR products of 16S rRNA gene were sequenced. Each 16S rRNA sequence was blasted against nucleotide database of NCBI to identify bacterial strains. The identified aerobic strains were preserved in 50% glycerol and anaerobic strains in 50% glycerol and 0.1% cysteine at -80°C freezer.

DNA extraction, whole-metagenome sequencing, and metagenomic analyses

The microbial DNA of gut content and fecal samples was extracted using Qiagen DNA extraction kit (Qiagen, Germany) according to the manufacturer's protocols. The DNA concentration and purity were quantified with TBS-380 and NanoDrop2000, respectively. DNA quality was examined with a 1% agarose gel electrophoresis system.

Metagenomic DNA was fragmented to an average size of ~300 bp using Covaris M220 (Gene Company Limited, China). Paired-end libraries were prepared by using a TruSeq DNA sample prep kit (Illumina, USA). Adapters containing the full complement of sequencing primer hybridization sites were ligated to blunt-end fragments. Paired-end sequencing was performed on Illumina HiSeq platform. High-quality reads were extracted based on the FASTQ (43), with default parameters. After then, sequencing reads with >90% similarity to the mouse genomic DNA were removed based on Bowtie2 alignment (44).

A gene catalogue was constructed based on the whole-metagenome sequencing data from the mouse gut samples. High-quality reads were used for *de novo* assembly via MEGAHIT (45), using different k-mer sizes (k = 21, 33, 55, 77). Gene identification was performed for all assembled scaffolds using MetaGeneMark(46). Predicted genes were clustered at the nucleotide level by CD-HIT (47), and genes sharing greater than 90% overlap and greater than 95% identity were treated as redundancies. Taxonomic assignment of the genes was generated by blasting against the NCBI-NT database. When alignments with >70% coverage, genes with >90% and sequence similarity >80% were used for species- and genus-level taxonomical annotation, respectively.

Metagenome-assembled genome (MAG)

To reconstructed the microbial genome from the metagenomic sequenced samples of mouse gut, we implied the methodology of metagenome-assembled genome that was recently developed by recent studies (18, 48). Briefly, sequenced reads were firstly mapped into the assembled contigs (>2,000bp) with Bowtie2 (44) to generate the mean coverage of contigs. Draft metagenome-assembled genomes were then independently recovered from the contigs of each sample using MetaBAT2 (49) under default parameters, based on the coverage and intrinsic information (e.g. GC content, tetranucleotide frequency) of contigs. The completeness and contamination of the raw MAGs were estimated using CheckM(50), and only MAGs fit the quality criteria of estimated completeness of >70% and contamination of<5% were kept. The pairwise average nucleotide identity (ANI) of MAGs was calculated using FastANI(51), and two MAGs with >95% of ANI were treated as redundancy. Finally, taxonomic assignment of MAGs was performed based on both SpecI (an accurate and universal delineation of prokaryotic species based on marker gene-based algorithm) (52) and whole-genome alignment against the NCBI sequenced bacterial genomes.

Comparison genomic analyses

Phylogenetic analysis of the genomes was carried out using the maximum-likelihood program RAxML(53) with a GTR model of evolution, and visualized on the iTOL web service (54). Robustness of the phylogenetic tree was estimated by bootstrap analysis in 1,000 replicates. The Kyoto Encyclopedia of Genes and Genomes (KEGG) and carbohydrate active enzymes (CAZymes) databases were used for functional annotation of genomes. For each genome, the protein-coding genes were assigned a KEGG orthologue or CAZyme on the basis of the best-hit gene in the databases.

Data availability

The raw sequencing data and metagenome-assembled genome sequences reported in this article have been deposited in the NCBI BioProjectPRJNA000000.

Acknowledgment

This work was supported by National Natural Science Foundation of China (81573469, 81930112, 81902037) and Natural Science Foundation of Liaoning Province, China (20180530086).

References

1. Richard ML, Sokol H. 2019. The gut mycobiota: insights into analysis, environmental interactions and role in gastrointestinal diseases. Nat Rev Gastroenterol Hepatol 16:331-345.
2. Le Chatelier E, Nielsen T, Qin J, Prifti E, Hildebrand F, Falony G, Almeida M, Arumugam M, Batto JM, Kennedy S, Leonard P, Li J, Burgdorf K, Grarup N, Jorgensen T, Brandslund I, Nielsen HB, Juncker AS, Bertalan M, Levenez F, Pons N, Rasmussen S, Sunagawa S, Tap J, Tims S, Zoetendal EG, Brunak S, Clement K, Dore J, Kleerebezem M, Kristiansen K, Renault P, Sicheritz-Ponten T, de Vos WM, Zucker JD, Raes J, Hansen T, Meta HITc, Bork P, Wang J, Ehrlich SD, Pedersen O. 2013. Richness of human gut microbiome correlates with metabolic markers. Nature 500:541-6.
3. Ley RE, Turnbaugh PJ, Klein S, Gordon JI. 2006. Microbial ecology: human gut microbes associated with obesity. Nature 444:1022-3.
4. Qin J, Li Y, Cai Z, Li S, Zhu J, Zhang F, Liang S, Zhang W, Guan Y, Shen D, Peng Y, Zhang D, Jie Z, Wu W, Qin Y, Xue W, Li J, Han L, Lu D, Wu P, Dai Y, Sun X, Li Z, Tang A, Zhong S, Li X, Chen W, Xu R, Wang M, Feng Q, Gong M, Yu J, Zhang Y, Zhang M, Hansen T, Sanchez G, Raes J, Falony G, Okuda S, Almeida M, LeChatelier E, Renault P, Pons N, Batto JM, Zhang Z, Chen H, Yang R, Zheng W, Li S, Yang H, et al. 2012. A metagenome-wide association study of gut microbiota in type 2 diabetes. Nature 490:55-60.
5. Vaahtovuo J, Munukka E, Korkeamaki M, Luukkainen R, Toivanen P. 2008. Fecal microbiota in early rheumatoid arthritis. J Rheumatol 35:1500-5.
6. Russell SL, Gold MJ, Hartmann M, Willing BP, Thorson L, Wlodarska M, Gill N, Blanchet MR, Mohn WW, McNagny KM, Finlay BB. 2012. Early life antibiotic-driven changes in microbiota enhance susceptibility to allergic asthma. EMBO Rep 13:440-7.
7. Tlaskalova-Hogenova H, Stepankova R, Kozakova H, Hudcovic T, Vannucci L, Tuckova L, Rossmann P, Hrncir T, Kverka M, Zakostelska Z, Klimesova K, Pribylova J, Bartova J, Sanchez D, Fundova P, Borovska D, Srutkova D, Zidek Z, Schwarzer M, Drastich P, Funda DP. 2011. The role of gut microbiota (commensal bacteria) and the mucosal barrier in the pathogenesis of inflammatory and autoimmune diseases and cancer: contribution of germ-free and gnotobiotic animal models of human diseases. Cell Mol Immunol 8:110-20.
8. Adak A, Khan MR. 2019. An insight into gut microbiota and its functionalities. Cell Mol Life Sci 76:473-493.
9. Nguyen TL, Vieira-Silva S, Liston A, Raes J. 2015. How informative is the mouse for human gut microbiota research? Dis Model Mech 8:1-16.
10. Eckburg PB, Bik EM, Bernstein CN, Purdom E, Dethlefsen L, Sargent M, Gill SR, Nelson KE, Relman DA. 2005. Diversity of the human intestinal microbial flora. Science 308:1635-8.
11. Ley RE, Backhed F, Turnbaugh P, Lozupone CA, Knight RD, Gordon JI. 2005. Obesity alters gut

353 microbial ecology. Proc Natl Acad Sci U S A 102:11070-5.
354 12. Dumont BL. 2019. Significant Strain Variation in the Mutation Spectra of Inbred Laboratory Mice.
355 Mol Biol Evol 36:865-874.
356 13. Gu S, Chen D, Zhang JN, Lv X, Wang K, Duan LP, Nie Y, Wu XL. 2013. Bacterial community map-
357 ping of the mouse gastrointestinal tract. PLoS One 8:e74957.
358 14. Xiao L, Feng Q, Liang S, Sonne SB, Xia Z, Qiu X, Li X, Long H, Zhang J, Zhang D, Liu C, Fang Z,
359 Chou J, Glanville J, Hao Q, Kotowska D, Colding C, Licht TR, Wu D, Yu J, Sung JJ, Liang Q, Li J,
360 Jia H, Lan Z, Tremaroli V, Dworzynski P, Nielsen HB, Backhed F, Dore J, Le Chatelier E, Ehrlich
361 SD, Lin JC, Arumugam M, Wang J, Madsen L, Kristiansen K. 2015. A catalog of the mouse gut met-
362 agenome. Nat Biotechnol 33:1103-8.
363 15. Hildebrand F, Nguyen TL, Brinkman B, Yunta RG, Cauwe B, Vandenabeele P, Liston A, Raes J.
364 2013. Inflammation-associated enterotypes, host genotype, cage and inter-individual effects drive
365 gut microbiota variation in common laboratory mice. Genome Biol 14:R4.
366 16. Li J, Jia H, Cai X, Zhong H, Feng Q, Sunagawa S, Arumugam M, Kultima JR, Prifti E, Nielsen T,
367 Juncker AS, Manichanh C, Chen B, Zhang W, Levenez F, Wang J, Xu X, Xiao L, Liang S, Zhang D,
368 Zhang Z, Chen W, Zhao H, Al-Aama JY, Edris S, Yang H, Wang J, Hansen T, Nielsen HB, Brunak S,
369 Kristiansen K, Guarner F, Pedersen O, Dore J, Ehrlich SD, Meta HITC, Bork P, Wang J, Meta HITC.
370 2014. An integrated catalog of reference genes in the human gut microbiome. Nat Biotechnol
371 32:834-41.
372 17. Pan H, Guo R, Zhu J, Wang Q, Ju Y, Xie Y, Zheng Y, Wang Z, Li T, Liu Z, Lu L, Li F, Tong B, Xiao
373 L, Xu X, Li R, Yuan Z, Yang H, Wang J, Kristiansen K, Jia H, Liu L. 2018. A gene catalogue of the
374 Sprague-Dawley rat gut metagenome. Gigascience 7.
375 18. Pasolli E, Asnicar F, Manara S, Zolfo M, Karcher N, Armanini F, Beghini F, Manghi P, Tett A, Ghen-
376 si P, Collado MC, Rice BL, DuLong C, Morgan XC, Golden CD, Quince C, Huttenhower C, Segata
377 N. 2019. Extensive Unexplored Human Microbiome Diversity Revealed by Over 150,000 Genomes
378 from Metagenomes Spanning Age, Geography, and Lifestyle. Cell 176:649-662 e20.
379 19. Nayfach S, Shi ZJ, Seshadri R, Pollard KS, Kyrpides NC. 2019. New insights from uncultivated ge-
380 nomes of the global human gut microbiome. Nature 568:505-510.
381 20. Lagkouvardos I, Overmann J, Clavel T. 2017. Cultured microbes represent a substantial fraction of
382 the human and mouse gut microbiota. Gut Microbes 8:493-503.
383 21. Browne HP, Forster SC, Anonye BO, Kumar N, Neville BA, Stares MD, Goulding D, Lawley TD.
384 2016. Culturing of 'unculturable' human microbiota reveals novel taxa and extensive sporulation.
385 Nature 533:543-546.
386 22. Kanehisa M, Furumichi M, Tanabe M, Sato Y, Morishima K. 2017. KEGG: new perspectives on ge-
387 nomes, pathways, diseases and drugs. Nucleic Acids Res 45:D353-D361.
388 23. Lombard V, Golaconda Ramulu H, Drula E, Coutinho PM, Henrissat B. 2014. The carbohydrate-
389 active enzymes database (CAZy) in 2013. Nucleic Acids Res 42:D490-5.
390 24. Robertson BR, O'Rourke JL, Neilan BA, Vandamme P, On SL, Fox JG, Lee A. 2005. Mucispirillum

391 schaedleri gen. nov., sp. nov., a spiral-shaped bacterium colonizing the mucus layer of the gastroin-
392 testinal tract of laboratory rodents. Int J Syst Evol Microbiol 55:1199-204.
393 25. Derrien M, Vaughan EE, Plugge CM, de Vos WM. 2004. Akkermansia muciniphila gen. nov., sp.
394 nov., a human intestinal mucin-degrading bacterium. Int J Syst Evol Microbiol 54:1469-76.
395 26. Alneberg J, Karlsson CMG, Divne AM, Bergin C, Homa F, Lindh MV, Hugerth LW, Ettema TJG,
396 Bertilsson S, Andersson AF, Pinhassi J. 2018. Genomes from uncultivated prokaryotes: a comparison
397 of metagenome-assembled and single-amplified genomes. Microbiome 6:173.
398 27. Bowers RM, Kyrpides NC, Stepanauskas R, Harmon-Smith M, Doud D, Reddy TBK, Schulz F, Jar-
399 ett J, Rivers AR, Eloe-Fadrosh EA, Tringe SG, Ivanova NN, Copeland A, Clum A, Becraft ED,
400 Malmstrom RR, Birren B, Podar M, Bork P, Weinstock GM, Garrity GM, Dodsworth JA, Yooseph S,
401 Sutton G, Glockner FO, Gilbert JA, Nelson WC, Hallam SJ, Jungbluth SP, Ettema TJG, Tighe S,
402 Konstantinidis KT, Liu WT, Baker BJ, Rattei T, Eisen JA, Hedlund B, McMahon KD, Fierer N,
403 Knight R, Finn R, Cochrane G, Karsch-Mizrachi I, Tyson GW, Rinke C, Genome Standards C, Lapi-
404 dus A, Meyer F, Yilmaz P, Parks DH, et al. 2017. Minimum information about a single amplified ge-
405 nome (MISAG) and a metagenome-assembled genome (MIMAG) of bacteria and archaea. Nat Bio-
406 technol 35:725-731.
407 28. Rosshart SP, Vassallo BG, Angeletti D, Hutchinson DS, Morgan AP, Takeda K, Hickman HD,
408 McCulloch JA, Badger JH, Ajami NJ, Trinchieri G, Pardo-Manuel de Villena F, Yewdell JW, Re-
409 hermann B. 2017. Wild Mouse Gut Microbiota Promotes Host Fitness and Improves Disease Re-
410 sistance. Cell 171:1015-1028 e13.
411 29. Robertson SJ, Goethel A, Girardin SE, Philpott DJ. 2018. Innate Immune Influences on the Gut Mi-
412 crobiome: Lessons from Mouse Models. Trends Immunol 39:992-1004.
413 30. Schwab C, Berry D, Rauch I, Rennisch I, Ramesmayer J, Hainzl E, Heider S, Decker T, Kenner L,
414 Muller M, Strobl B, Wagner M, Schleper C, Loy A, Urich T. 2014. Longitudinal study of murine mi-
415 crobiota activity and interactions with the host during acute inflammation and recovery. ISME J
416 8:1101-14.
417 31. Berry D, Schwab C, Milinovich G, Reichert J, Ben Mahfoudh K, Decker T, Engel M, Hai B, Hainzl
418 E, Heider S, Kenner L, Muller M, Rauch I, Strobl B, Wagner M, Schleper C, Urich T, Loy A. 2012.
419 Phylotype-level 16S rRNA analysis reveals new bacterial indicators of health state in acute murine
420 colitis. ISME J 6:2091-106.
421 32. Robertson SJ, Geddes K, Maisonneuve C, Streutker CJ, Philpott DJ. 2016. Resilience of the intesti-
422 nal microbiota following pathogenic bacterial infection is independent of innate immunity mediated
423 by NOD1 or NOD2. Microbes Infect 18:460-71.
424 33. Barcenilla A, Pryde SE, Martin JC, Duncan SH, Stewart CS, Henderson C, Flint HJ. 2000. Phyloge-
425 netic relationships of butyrate-producing bacteria from the human gut. Appl Environ Microbiol
426 66:1654-61.
427 34. Pryde SE, Duncan SH, Hold GL, Stewart CS, Flint HJ. 2002. The microbiology of butyrate for-
428 mation in the human colon. FEMS Microbiol Lett 217:133-9.

35. Schleifer KH, Kandler O. 1972. Peptidoglycan types of bacterial cell walls and their taxonomic implications. Bacteriol Rev 36:407-77.

36. Schleifer KH. 2009. Classification of Bacteria and Archaea: past, present and future. Syst Appl Microbiol 32:533-42.

37. Xing J, Li X, Sun Y, Zhao J, Miao S, Xiong Q, Zhang Y, Zhang G. 2019. Comparative genomic and functional analysis of Akkermansia muciniphila and closely related species. Genes Genomics 41:1253-1264.

38. Presley LL, Wei B, Braun J, Borneman J. 2010. Bacteria associated with immunoregulatory cells in mice. Appl Environ Microbiol 76:936-41.

39. Hansen CH, Krych L, Nielsen DS, Vogensen FK, Hansen LH, Sorensen SJ, Buschard K, Hansen AK. 2012. Early life treatment with vancomycin propagates Akkermansia muciniphila and reduces diabetes incidence in the NOD mouse. Diabetologia 55:2285-94.

40. Png CW, Linden SK, Gilshenan KS, Zoetendal EG, McSweeney CS, Sly LI, McGuckin MA, Florin TH. 2010. Mucolytic bacteria with increased prevalence in IBD mucosa augment in vitro utilization of mucin by other bacteria. Am J Gastroenterol 105:2420-8.

41. Wang L, Christophersen CT, Sorich MJ, Gerber JP, Angley MT, Conlon MA. 2011. Low relative abundances of the mucolytic bacterium Akkermansia muciniphila and Bifidobacterium spp. in feces of children with autism. Appl Environ Microbiol 77:6718-21.

42. Weir TL, Manter DK, Sheflin AM, Barnett BA, Heuberger AL, Ryan EP. 2013. Stool microbiome and metabolome differences between colorectal cancer patients and healthy adults. PLoS One 8:e70803.

43. Chen S, Zhou Y, Chen Y, Gu J. 2018. fastp: an ultra-fast all-in-one FASTQ preprocessor. Bioinformatics 34:i884-i890.

44. Langmead B, Salzberg SL. 2012. Fast gapped-read alignment with Bowtie 2. Nat Methods 9:357-9.

45. Li D, Liu CM, Luo R, Sadakane K, Lam TW. 2015. MEGAHIT: an ultra-fast single-node solution for large and complex metagenomics assembly via succinct de Bruijn graph. Bioinformatics 31:1674-6.

46. Zhu W, Lomsadze A, Borodovsky M. 2010. Ab initio gene identification in metagenomic sequences. Nucleic Acids Res 38:e132.

47. Li W, Godzik A. 2006. Cd-hit: a fast program for clustering and comparing large sets of protein or nucleotide sequences. Bioinformatics 22:1658-9.

48. Parks DH, Rinke C, Chuvochina M, Chaumeil PA, Woodcroft BJ, Evans PN, Hugenholtz P, Tyson GW. 2017. Recovery of nearly 8,000 metagenome-assembled genomes substantially expands the tree of life. Nat Microbiol 2:1533-1542.

49. Kang DD, Li F, Kirton E, Thomas A, Egan R, An H, Wang Z. 2019. MetaBAT 2: an adaptive binning algorithm for robust and efficient genome reconstruction from metagenome assemblies. PeerJ 7:e7359.

50. Parks DH, Imelfort M, Skennerton CT, Hugenholtz P, Tyson GW. 2015. CheckM: assessing the qual-

ity of microbial genomes recovered from isolates, single cells, and metagenomes. Genome Res 25:1043-55.

51. Jain C, Rodriguez RL, Phillippy AM, Konstantinidis KT, Aluru S. 2018. High throughput ANI analysis of 90K prokaryotic genomes reveals clear species boundaries. Nat Commun 9:5114.

52. Mende DR, Sunagawa S, Zeller G, Bork P. 2013. Accurate and universal delineation of prokaryotic species. Nat Methods 10:881-4.

53. Stamatakis A. 2014. RAxML version 8: a tool for phylogenetic analysis and post-analysis of large phylogenies. Bioinformatics 30:1312-3.

54. Letunic I, Bork P. 2016. Interactive tree of life (iTOL) v3: an online tool for the display and annotation of phylogenetic and other trees. Nucleic Acids Res 44:W242-5.

Table 1. Summary of genomic characteristics of Bacteroidetes and Firmicutes strains derived from the human and mouse gut microbiota.

	No. of genomes	**Genome size (Mbp)***	**No. of genes***	**% GC content**	**No. of KEGG orthologs**	**No. of CAZy proteins**
Bacteroidetes						
Human strains	31	5.1±1.1	4,348±908	44.8±4.0	1558±271	357±178
Mouse MAGs	22	2.9±0.8	2,637±795	50.2±3.3	992±176	122±49
P value		1.8×10^{-11}	2.6×10^{-19}	1.9×10^{-6}	2.1×10^{-12}	3.3×10^{-8}
Firmicutes						
Human strains	175	3.7±1.1	3,474±1,110	43.0±8.1	1554±455	111±87
Mouse MAGs	23	3.4±0.8	3,350±702	45.5±6.2	1274±224	104±46
P value		0.122	0.464	0.094	6.7×10^{-6}	0.544

Note: * the genome size and number of genes of mouse MAGs were estimated based on their completeness.

Figure legend

Figure 1. Gene catalogue and microbial community composition of the mouse gut microbiota. (A) Comparison of the fecal gene catalogue, the gut content gene catalogue, and the available mouse gut gene catalogue established by 184 mice faeces. **(B)** Microbial community composition of the mouse gut microbiota at the phylum and genus levels. **(C)** Gene sharing relationship of the mouse, rat and human gut microbial gene catalogues.

Figure 2. Detailed information and validation of MAGs reconstructed from the mouse gut. (A) Summary information of 55 nonredundant MAGs. **(B)** Circular representation of draft genome of a *Lactobacillus murinus* strain isolated from the mouse gut. The inner two circles represent the GC skew and GC content of the *L. murinus* MS13 genome. The outer two circles show the homologous comparison of *L. murinus* MS13 with *L. murinus* MAG:BG01 (reconstructed from the mouse gut) and *L. murinus* CR141 (the closest strain from the NCBI sequenced genomes).

Figure 3. Comparison of Bacteroidetes and Firmicutes strains between mouse and human guts. (A) Phylogenetic tree of 55 mouse MAGs and 206 human gut genomes. The outer circle indicates the phylum level taxonomy of the genomes, and the inner circle indicates their host. **(B)** Principle coordination analysis shows the functional difference of Bacteroidetes and Firmicutes strains between mouse and human guts. Isolates on the first and second principal components are plotted by nodes. Lines connect isolates in the same groups, and colored circles cover the isolates near the center of gravity for each group. **(C)** Box-plot shows the difference of flagella assembly and bacterial chemotaxis in the mouse Firmicutes strains compared to human strains.

Figure 4. Representative strains in the mouse gut microbiota. Circular representation of draft genome of four representative strains, including *Mucispirillumschaedleri*MAG:AF02 **(A)**, *Parasutterella excrementihominis* MAG:CG14 **(B)**, *Helicobacter typhlonius* MAG:AF12 **(C)**, and *Akkermansia muciniphila* MAG:BG08 **(D)**, in the mouse gut microbiota. The inner two circles represent the GC skew and GC content

of the genomes, and the outer circle shows the comparison of the genome with the highest homologous strains from NCBI database.

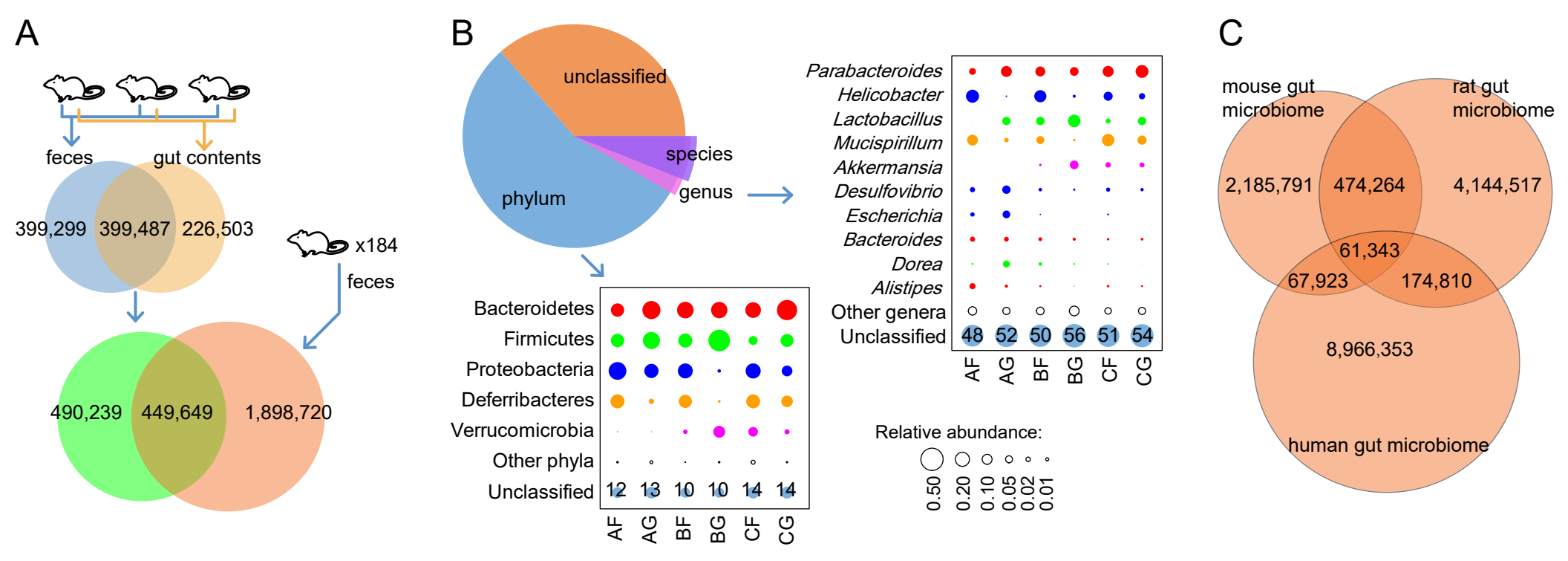
A
feces
gut contents
399,299
399,487
226,503
x184
feces
490,239
449,649
1,898,720
B
unclassified
species
genus
phylum
Parabacteroides
Helicobacter
Lactobacillus
Mucispirillum
Akkermansia
Desulfovibrio
Escherichia
Bacteroides
Dorea
Alistipes
Other genera
Unclassified
48
52
50
56
51
54
AF
AG
BF
BG
CF
CG
Bacteroidetes
Firmicutes
Proteobacteria
Deferribacteres
Verrucomicrobia
Other phyla
Unclassified
12
13
10
10
14
14
AF
AG
BF
BG
CF
CG
Relative abundance:
0.50
0.20
0.10
0.05
0.02
0.01
C
mouse gut microbiome
rat gut microbiome
2,185,791
474,264
4,144,517
61,343
67,923
174,810
8,966,353
human gut microbiome

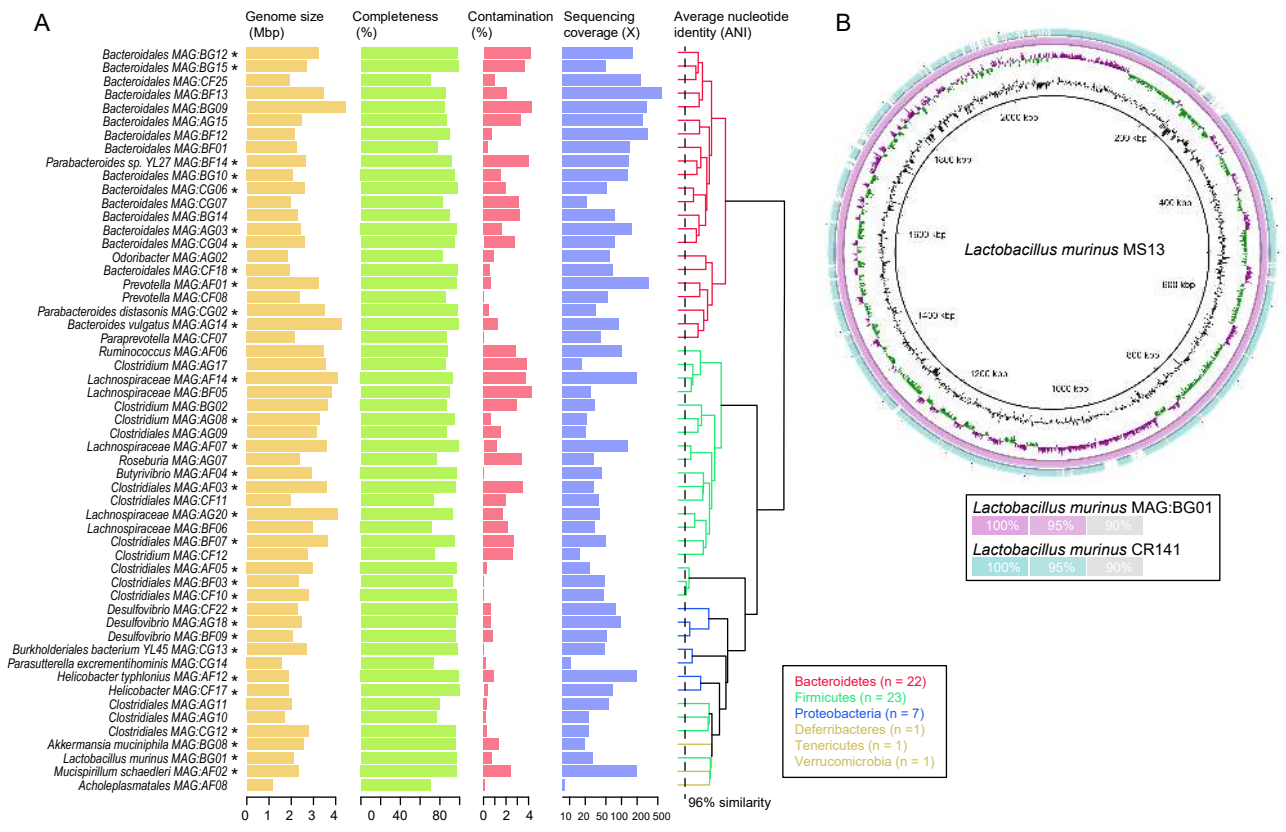
A
Genome size (Mbp)
Completeness (%)
Contamination (%)
Sequencing coverage (X)
Average nucleotide identity (ANI)
Bacteroidales MAG:BG12 *
Bacteroidales MAG:BG15 *
Bacteroidales MAG:CF25
Bacteroidales MAG:BF13
Bacteroidales MAG:BG09
Bacteroidales MAG:AG15
Bacteroidales MAG:BF12
Bacteroidales MAG:BF01
Parabacteroides sp. YL27 MAG:BF14 *
Bacteroidales MAG:BG10 *
Bacteroidales MAG:CG06 *
Bacteroidales MAG:CG07
Bacteroidales MAG:BG14
Bacteroidales MAG:AG03 *
Bacteroidales MAG:CG04 *
Odoribacter MAG:AG02
Bacteroidales MAG:CF18 *
Prevotella MAG:AF01 *
Prevotella MAG:CF08
Parabacteroides distasonis MAG:CG02 *
Bacteroides vulgatus MAG:AG14 *
Paraprevotella MAG:CF07
Ruminococcus MAG:AF06
Clostridium MAG:AG17
Lachnospiraceae MAG:AF14 *
Lachnospiraceae MAG:BF05
Clostridium MAG:BG02
Clostridium MAG:AG08 *
Clostridiales MAG:AG09
Lachnospiraceae MAG:AF07 *
Roseburia MAG:AG07
Butyrivibrio MAG:AF04 *
Clostridiales MAG:AF03 *
Clostridiales MAG:CF11
Lachnospiraceae MAG:AG20 *
Lachnospiraceae MAG:BF06
Clostridiales MAG:BF07 *
Clostridium MAG:CF12
Clostridiales MAG:AF05 *
Clostridiales MAG:BF03 *
Clostridiales MAG:CF10 *
Desulfovibrio MAG:CF22 *
Desulfovibrio MAG:AG18 *
Desulfovibrio MAG:BF09 *
Burkholderiales bacterium YL45 MAG:CG13 *
Parasutterella excrementihominis MAG:CG14
Helicobacter typhlonius MAG:AF12 *
Helicobacter MAG:CF17 *
Clostridiales MAG:AG11
Clostridiales MAG:AG10
Clostridiales MAG:CG12 *
Akkermansia muciniphila MAG:BG08 *
Lactobacillus murinus MAG:BG01 *
Mucispirillum schaedleri MAG:AF02 *
Acholeplasmatales MAG:AF08
0 1 2 3 4
0 40 80
0 2 4
10 20 50 100 200 500
96% similarity
Bacteroidetes (n = 22)
Firmicutes (n = 23)
Proteobacteria (n = 7)
Deferribacteres (n =1)
Tenericutes (n = 1)
Verrucomicrobia (n = 1)
B
2000 kbp
200 kbp
1800 kbp
400 kbp
1600 kbp
Lactobacillus murinus MS13
600 kbp
1400 kbp
800 kbp
1200 kbp
1000 kbp
Lactobacillus murinus MAG:BG01
100%
95%
90%
Lactobacillus murinus CR141
100%
95%
90%

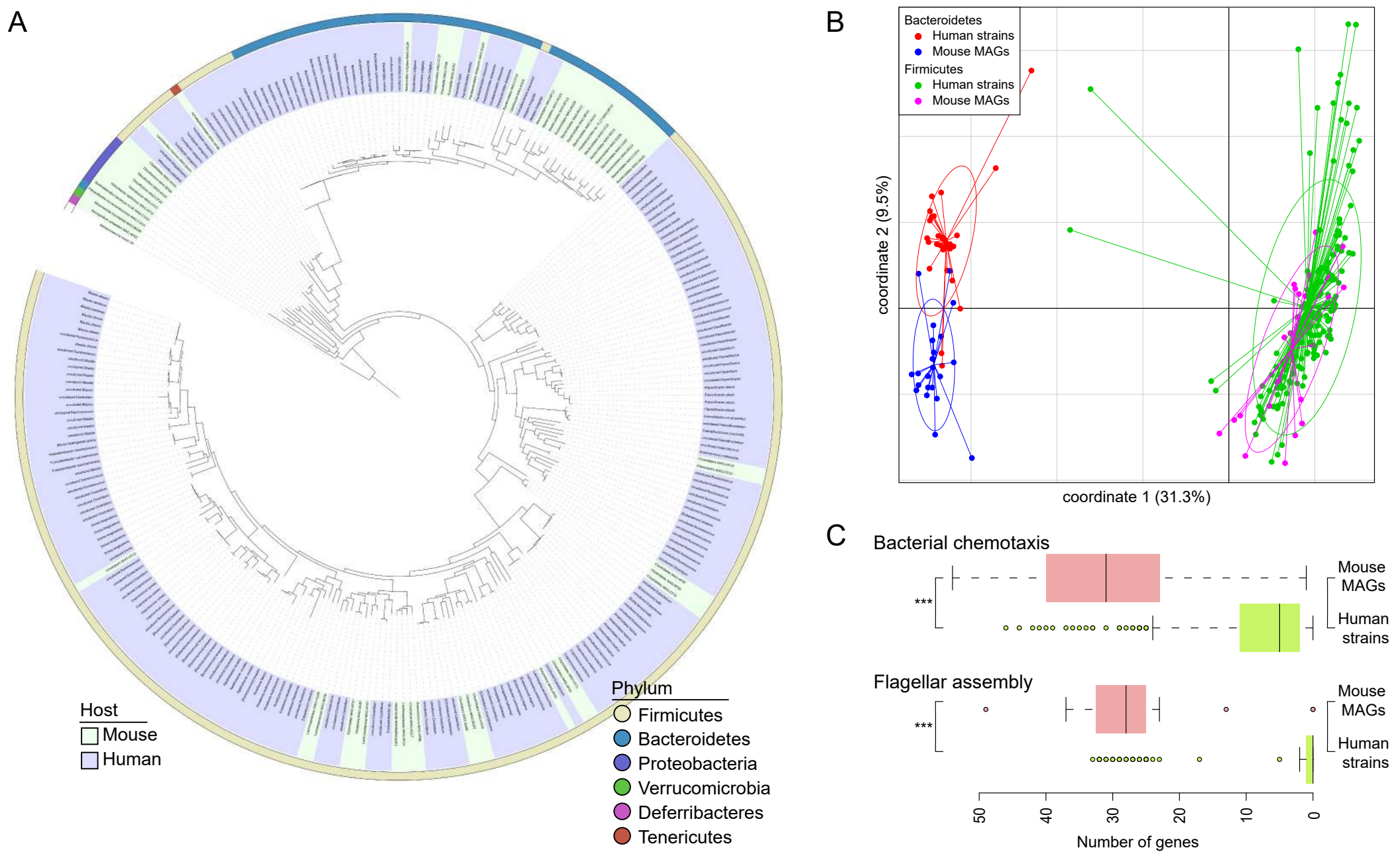
A
Host
Mouse
Human
Phylum
Firmicutes
Bacteroidetes
Proteobacteria
Verrucomicrobia
Deferribacteres
Tenericutes
B
Bacteroidetes
Human strains
Mouse MAGs
Firmicutes
Human strains
Mouse MAGs
coordinate 2 (9.5%)
coordinate 1 (31.3%)
C
Bacterial chemotaxis
***
Mouse MAGs
Human strains
Flagellar assembly
***
Mouse MAGs
Human strains
50
40
30
20
10
0
Number of genes

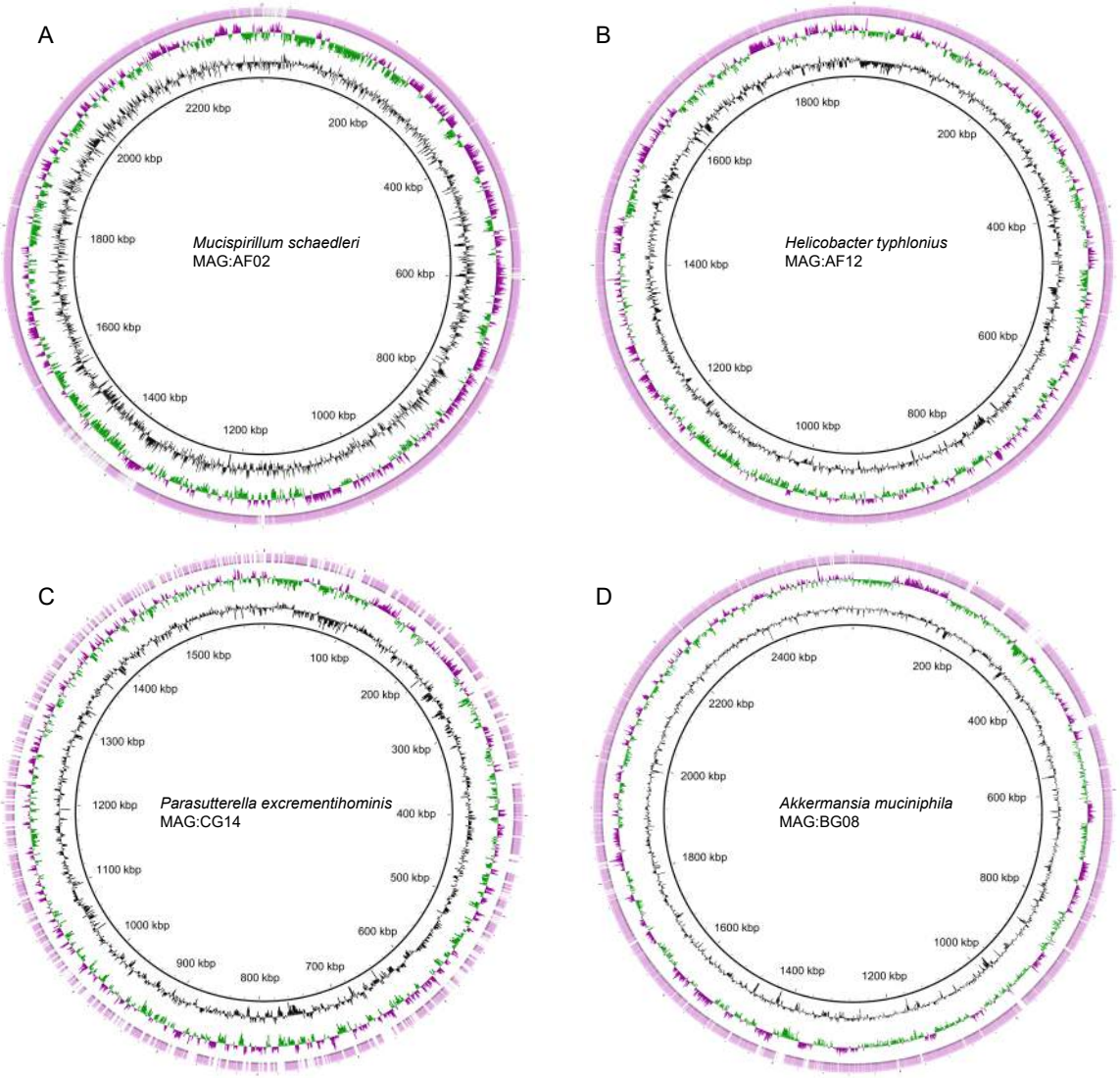
A
2200 kbp
200 kbp
2000 kbp
400 kbp
1800 kbp
Mucispirillum schaedleri
MAG:AF02
600 kbp
1600 kbp
800 kbp
1400 kbp
1000 kbp
1200 kbp
B
1800 kbp
200 kbp
1600 kbp
400 kbp
1400 kbp
Helicobacter typhlonius
MAG:AF12
600 kbp
1200 kbp
800 kbp
1000 kbp
C
1500 kbp
100 kbp
1400 kbp
200 kbp
1300 kbp
300 kbp
1200 kbp
Parasutterella excrementihominis
MAG:CG14
400 kbp
1100 kbp
500 kbp
1000 kbp
600 kbp
900 kbp
700 kbp
800 kbp
D
2400 kbp
200 kbp
2200 kbp
400 kbp
2000 kbp
600 kbp
Akkermansia muciniphila
MAG:BG08
1800 kbp
800 kbp
1600 kbp
1000 kbp
1400 kbp
1200 kbp